Classification of Flow Regimes Using Linear Discriminant Analysis (LDA) and Support Vector Machine (SVM).

M. Tech Thesis

Submitted by

Anil Kumar Singh

(Roll No. 211CH1040)

Submitted in partial fulfillment for the degree of

Master of Technology (2011-13)

Under the Guidance of

Prof. Madhusree Kundu

Department of Chemical Engineering

National Institute of Technology

Rourkela769008

Orissa

May, 2013

ACKNOWLEDGEMENT

NATIONAL INSTITUTE OF TECHNOLOGY, ROURKELA

CERTIFICATE

This is to certify that the thesis entitled, "**Classification of Flow Regimes Using Linear Discriminant Analysis (LDA) and Support Vector Machine (SVM).**" submitted by Anil Kumar Singh**,** Roll No - 211CH1040 forthe award of the Master of Technology Degree in Chemical Engineering (2011-13) at National Institute of Technology, Rourkela. The candidate has fulfilled all prescribed requirements and the thesis, which is based on candidate's own work, has not been submitted elsewhere.

(Prof. Madhusree Kundu)

Department of Chemical Engineering

Content   **Page No.**

*List of figures***:**

*Appendices***:**

*Abbreviations***:**

b	*Bias or Threshold value*
C	*Regularization parameter, Tradeoff cost*
C_L	*Liquid coefficient constant in friction factor correlation*
$(dp/dx)_{LS}$	*Pressure drop of liquid phase flowing alone in pipe, N/m^2*
D	*Pipe diameter, m*
Fr	*Froude number (proportional to the inertial force/ gravitational force)*
$f(x)$	*Output of decision function, +1 or -1*
g	*Acceleration due to gravity, m/s^2*
P,p	*Degree of polynomial kernel function*
w	*Weight vector representing the level of influence on the input*
x	*Input attributes*
y_i	*Class of data point,+1or-1*
Ar	*Modified Archimedes number*

d_p	Particle diameter, mm
f	Friction factor
g	Acceleration due to gravity, m/s^2
H	Total bed height, m
H_c	Height of the column, m
H_f	Height of fluidized bed, m
H_o	Height of initial bed, m
H_p	Height of the packed bed, m
Re	Reynolds number, $d_p \rho_L U_1 / \mu_L$
Re_m	Modified Reynolds number, $d_p \rho_L U_1 / \mu_L (1 - \epsilon_p)$
U_1	Superficial liquid velocity, m/s
U_{mf}	Minimum fluidization velocity, m/s
U_{of}	Onset fluidization velocity, m/s

Greek Symbols

α	Specific flow pattern accuracy rate
α_i	Lagrange multipliers
β	Overall flow regime model accuracy rate
ρ_L, ρ_G	Gas and Liquid densities, respectively, kg/m^3
$\Delta\rho$	$(\rho_L - \rho_G)$, kg/m^3
μ_L, μ_G	Gas and Liquid viscosities, respectively, kg/m-s
σ	Surface Tension, N/m
ϵ_p, ϵ_f	Voidage of Packed bed and Fluidized bed

Abstract

This dissertation project presents a novel method for the classification of vertical and horizontal two-phase flow regimes through pipes. For gas-liquid vertical and horizontal two-phase flows, the goal of the study is to predict the transition region between the flow regimesusing the data generated by empirical correlations. The transition region is determined with respect to pipe diameter, superficial gas velocity, and superficial liquid velocity. Accurate determination of the flow regime is critical in the design of multiphase flow systems, which are used in various industrial processes, including boiling and condensation, oil and gas pipelines, and cooling systems for nuclear reactors.

Hydrodynamic characteristics of a new mode of liquid-solid fluidization, termed as "inverse fluidization" in which low density floating particles are fluidized with downward flow of liquid, are investigated. During the operation, three regimes, namely, packed, semi-fluidization and fully fluidization are encountered. With the help of proposedempirical correlations different flow regimes have been simulated with respect to the varying pressure drop across the bed with changing liquid velocity.Inverse fluidization finds main application in environmental engineering for waste water treatment and in biochemical engineering and biological reactors, and a proper specification of the fluidized bed regime is required.

One more study is concerned about gas fluidized beds. Gas fluidization is a very important process as it is used in many chemical engineering plant such as nuclear power stations, polymer industries etc. Sometimes quality of the fluidization in gas fluidized beds is affected by changing the diameter and densities of the particle for a specified flow regime.

Theflow through pipes, inverted fluidized beds and gas fluidized beds has one commonality; there prevail different flow regimes and the classification among them isbeingaccomplishedhere with the application of Chemometrics techniques.Two Chemometrics techniques are used for the classification of different flow regimes encountered in all of the aforesaid situations namely, Linear Discriminant Analysis (LDA) and Support Vector Machine (SVM). Using LDA both binary and multi-classification is done. When the SVM used, the support vectors of the concerned hydrodynamic data are identified and used to determine the transition zone between the multiphase flow patterns and between fluidized bed regimes. The models proved to be an accurate classification tool for the identification of flow regimes.

Chapter 1
Introduction

1.1   Introduction

This chapter introduces the project. A brief theoretical description and industrial significance of flow regimes pertainin two phase flow through pipes,inverted fluidized bed and gas fluidized bed is presented here. Later on, a small detail of the characterization and classification techniques Linear Discriminant Analysis (LDA) and Support Vector Machine (SVM)are discussed.

1.2   Multiphase flow

Multiphase flow is the simultaneous flow of two or more phases in a conduit. The simultaneous flow causes certain flow patterns to evolve depending on the pipe size, the flow rates, the fluid properties, and the pipe inclination angle (when appropriate). Accurate determination of the flow regime is critical in the design of multiphase flow systems, which are used in various industrial processes, including boiling and condensation, oil and gas pipelines, and cooling systems for nuclearreactors.The problem of identifying flow regimes is the result of a lack of universal delineation criteria for the transition zones from one pattern to the other. Considerable progress has been made in defining flow patterns **[1, 2];** however, there is no exact theory for the characterization of these patterns. Furthermore, the subjective character of the flow pattern identification often causes disagreements between researchers. While there is agreement on the existence of several flow patterns, there is often disagreement about the delineation point transition boundaries for each flow pattern. Such disagreements make the selection of an appropriate flow correlation a complicated issue. Mechanistic models are theoretical models that incorporate important variables coupled with state-of-the-art laboratory facilities for experiments. While mechanistic models offer an improvement in the understanding of multiphase flow systems, they are limited by the unavailability of precise solutions for the identification of different flow regimes. For most of the flow patterns observed, one or more empirical, closed-form relationships are required, even when a mechanistic approach is used. Therefore, it is important to develop a flow pattern model which minimizes the rate of misclassification errors (i.e., errors of predicting the wrong flow regime for a given set of flow

data) as well as extends the applicability of any new multiphase flow correlation to different pipe sizes, flow rates, and fluid properties.

1.3   Inverse Fluidization

Inverse fluidization is a technique in which solid particles having lower density than that of the liquid, are kept in suspension by the downward flow of continuous liquid phase. An important application of liquid-solid fluidized beds has been developed recently in biotechnology, namely, immobilized biocatalyst bioreactors **[3]**. Inverse fluidization finds main application in environmental engineering for waste water treatment and in biochemical engineering and biological reactors. In inverse fluidized bed there are mainly three regimes for the bed while operation namely as the packed bed regime, semi-fluidized regime and fully fluidized regime. Here also an accurate determination of all the regimes is required.

1.4   Effect of diameter and density variation on fluidization in gas fluidized bed

In chemical engineering operations gas fluidization has its own importance as it is used in many processes where the perfect quality of fluidization is required. In the study it is shown that for a particular fluidization we can use a range of different materials and required fluidization is achieved. Though different materials can be used for a specified fluidization regime but there is an appreciable effect of changing the density and diameter of the fluidization particle. This observation is also important to have the appropriate operation.

On the basis of the diameter and density fluidization particles are grouped mainly in four groups named as Geldart on the name of *Professor D. Geldart*, who named it. Design methods for fluidized beds can be tailored based upon the particle's Geldart grouping.

Group A For this group the particle size is between 20 and 100 μm, and the particle density is typically less than 1.4g/cm^3. Prior to the initiation of a bubbling bed phase, beds from these particles will expand by a factor of 2 to 3 at incipient fluidization, due to a decreased bulk density. Most powder-catalysed beds utilize this group.

Group B The particle size lies between 40 and 500 µm and the particle density between 1.4-4g/cm^3. Bubbling typically forms directly at incipient fluidization.

Group C This group contains extremely fine and consequently the most cohesive particles. With a size of 20 to 30 µm, these particles fluidize under very difficult to achieve conditions, and may require the application of an external force, such as mechanical agitation.

Group D The particles in this region are above 600 µm and typically have high particle densities. Fluidization of this group requires very high fluid energies and is typically associated with high levels of abrasion. Drying grains and peas, roasting coffee beans, gasifying coals, and some roasting metal ores are such solids, and they are usually processed in shallow beds or in the spouting mode.

We have taken the particles of Geldart B and A for the study.

1.5   Chemometric Techniques

Chemometrics is the science of extracting information from chemical systems by data-driven means. It is a highly interfacial discipline, using methods frequently employed in core data-analytic disciplines such as multivariate statistics, applied mathematics and computer science, in order to address problems in chemistry, biochemistry, medicine, biology and chemical engineering. Some large chemometric application areas have gone on to represent new domains, such as molecular modeling and QSAR, cheminformatics, the '-omics' fields of genomics, proteomics, metabonomics and metabolomics, process modeling and process analytical technology. The field is generally recognized to have emerged in the 1970s as computers became increasingly exploited for scientific investigation. The term 'chemometrics' was coined by SvanteWold in 1971, and the International Chemometrics Society was formed shortly thereafter by SvanteWold and Bruce Kowalski, two pioneers in the field.

Multivariate analysis was a critical facet even in the earliest applications of chemometrics. Two such techniques, namely LDA and SVM are used in this study for the discrimination purpose.

1.5.1 Linear Discriminant Analysis (LDA)

This type of approach involves maximizing the ratio of between class variance to within class variance. The main objective is to maximize this ratio so that adequate class separability is obtained. The class-specific type approach involves using two optimizing criteria for transforming the data sets independently. LDA perform dimensionality reduction, seeks to find directions along which the classes are best separated and takes into consideration the scatter within-classesbut also the scatter between-classes.

1.5.2 Support Vector Machine (SVM)

Support Vector Machines, are supervised learning machines based on statistical learning theorythat can be used for pattern recognition and regression. In this work SVM is used to make clear cut decision boundaries among different flow regimes. Statistical learning theory can identify rather precisely the factors that need to be taken into account to learn successfully certain simple types of algorithms, however, real-world applications usually need more complex models and algorithms (such as neural networks), that makes them much harder to analyze theoretically. SVM can be seen as a linear algorithm in a high-dimensional space.

1.6 Objective of the Thesis

Following are the objectives of the present dissertation.
- ✓ To classify the flow regimes in two phase flow through pipes
- ✓ Classification amongflow regimes in invertedfluidized beds
- ✓ Classification among flow regimes in gas fluidized beds using the Geldart B and A fluidization particles
- ✓ The aforesaid classification among the prevailing flow regimes to be accomplished using two machine learning algorithms, namely, LDA and SVM.

1.7   Organization of the Thesis

Chapter 1 presents the brief account of the present dissertation with the objective and the thesis outline.

Chapter 2 renders theoretical postulations of the chemometric techniques which are used for classification.

Chapter 3 deals with the literature of Two Phase Flow through Pipe, correlations used for the generation of hydrodynamic dataand development of LDA and SVM classifiers for the same.

Chapter 4describes about the inverse fluidization and also has details about the correlation for data generation followed by the development of LDA and SVM classifiers for the same.

Chapter 5 describes about the gas fluidized bed details and the development of LDA and SVM classifiers for the same.

Chapter 6 deals with the conclusion and the recommendations of the project.

All the *references*, *appendices* are attached in the last of the thesis.

Chapter 2
Mathematical and Theoretical Postulation of LDA and SVM

This chapter deals with the theoretical and mathematical postulation of both the techniques, LDA and SVM.

2.1 LDA

There are many possible techniques for classification of data. Linear Discriminant Analysis (LDA) is commonly used technique for data classification and dimensionality reduction. Attempt to express one dependent variable as a linear combination of other features or measurements and the dependent variable for LDA is a categorical variable (*i.e.* the class label). Linear Discriminant Analysis easily handles the case where the within-class frequencies are unequal and their performances have been examined on randomly generated test data. This method maximizes the ratio of between-class variance to the within-class variance in any particular data set thereby guaranteeing maximal separability. The use of Linear Discriminant Analysis for data classification is applied to classification problem in patternrecognition. We decided to implement an algorithm for LDA in hopes of providing better classification compared to Principal components Analysis. LDA explicitly attempts to model the difference between the classes of data. PCA on the other hand does not take into account any difference in class. LDA doesn't change the location but only tries to provide more class separability and draw a decision region between the given classes. This method also helps to better understand the distribution of the feature data**[4]**.

2.1.1 Different approaches to LDA

Data sets can be transformed and test vectors can be classified in the transformed space by twodifferent approaches.

*2.1.1.1 Class-dependent transformation***:**

This type of approach involves maximizing the ratio of betweenclass variance to within class variance. The main objective is to maximize this ratio so that adequateclass separability is obtained. The

class-specific type approach involves using two optimizing criteriafor transforming the data sets independently.

2.1.1.2   *Class-independent transformation*:

This approach involves maximizing the ratio of overall varianceto within class variance. This approach uses only one optimizing criterion to transform the data setsand hence all data points irrespective of their class identity are transformed using this transform. Inthis type of LDA, each class is considered as a separate class against all other classes.

2.1.2   Mathematical Operation of LDA

In this section, the mathematical operations involved in using LDA will be analyzed.

1:   Formulate the data sets and the test sets, which are to be classified in the original space. For ease of understanding let us represent the data sets as a matrix consisting of features in the form given below:

$$Set\ 1\ =\ [\ a_{11}a_{21}\ ..... a_{m1},\ \ \ \ a_{12}a_{22}\ ..... a_{m2}]$$

$$Set\ 2\ =\ [\ b_{11}b_{21}\ ..... b_{m1},\ \ b_{12}b_{22}\ ..... b_{m2}] \hspace{2cm} 2.1$$

2:   Compute the mean of each data set and mean of entire data set. Let μ_1 and $\mu_2$be the mean of set 1 and set 2 respectively and μ_3 be mean of entire data, which is obtained by merging set 1 and set 2, is given by Equation 1.

$$\mu_3\ =\ p_1\ *\ \mu_1\ +\ p_2\ *\ \mu_2 \hspace{2cm} 2.2$$

Where p1and p2 are the apriori probabilities of the classes. In the case of this simple two class problem, the probability factor is assumed to be 0.5.

3: In LDA, within-class and between-class scatter are used to formulate criteria for classseparability. Within-class scatter is the expected covariance of each of the classes. The scatter measures are computed using Equations 3 and 4.

$$S_w = \Sigma \ p_j \ * \ (covj) \qquad\qquad 2.3$$

Therefore for two class problem

$$S_w = 0.5 * cov1 + 0.5 * cov2 \qquad\qquad 2.4$$

All the covariance matrices are symmetric. Let cov_1 and cov_2 be the covariance of set 1 and set 2 respectively. Covariance matrix is computed using the following equation.

$$covj = (x_j - \mu_j)(x_j - \mu_j)^T \qquad\qquad 2.5$$

The between-class scatter computes using the following equation.

$$Sb = \Sigma \ (\mu_j - \mu_3) * (\mu_j - \mu_3)^T \qquad\qquad 2.6$$

As defined earlier, the optimizing criterion in LDA is the ratio of between-class scatter to the within-class scatter. The solution obtained by maximizing this criterion defines the axes of the transformed space. However for the class-dependent transform the optimizing criterion is computed using equations 2.5 and 2.6. It should be noted that if theLDA is a class dependent type, forL-class separate optimizing criterion are required for each class. The optimizing factors in case of class dependent type are computed as

$$criterion = inv\,(covj)\,*\,S_b \qquad\qquad 2.7$$

For the class independent transform, the optimizing criterion is computed as

$$criterion = inv\,(S_w)\,*\,S_b \qquad\qquad 2.8$$

4: By definition, an Eigen vector of a transformation represents a 1-D invariant subspace of the vector space in which the transformation is applied. A set of these Eigen vectors whose corresponding Eigen values are non-zero are all linearly independent and are invariant under the transformation. Thus any vector space can be represented in terms of linear combinations of the Eigen vectors. A linear dependency between features is indicated by azero Eigen value. To obtain a non-redundant set of features all Eigen vectors corresponding to non-zero Eigen values only are considered and the ones corresponding to zero Eigenvalues are neglected. In the case of LDA, the transformations are found as the Eigen vector matrix of the different criteria defined in Equations 2.7 and 2.8.

5: For anyL-class problem we would always haveL-1non-zero Eigen values. This is attributed to the constraints on the mean vectors of the classes in eq. 2.2. The Eigen vectors corresponding to non-zero Eigen values for the definition of the transformation. For our 2-class example,having obtained the transformation matrices, we transform the data sets using the single LDA transform or the class specific transforms whichever the case may be. From the figures it can be observed that, transforming the entire data set to one axis provides definite boundaries to classify the data. The decision region in the transformed space is a solid line separating the transformed data sets thus for the class dependent LDA,

$$transform\_set\_j = transform\_j^T\,*\,set\_j^T \qquad\qquad 2.9$$

For the class independent LDA

$$transform\_set = transform\_spec^T * data\_set^T \qquad 2.10$$

Similarly the test vectors are transformed and are classified using the Euclidean distance of the test vectors from each class mean. The original data sets are shown and the same data sets after transformation are also illustrated. It is quite clear from these figures that transformation provides a boundary for proper classification. In this example the classes were properly defined but cases where there is overlap between classes, obtaining a decision region in original space will be very difficult and in such cases transformation proves to be very essential. Transformation along largest Eigenvector axis is the best transformation.

Mat Lab instructions for LDA is explained in *Appendix A*

2.2 SVM

The Support Vector Machine (SVM) is a technique for classification and regression. Originally the SVM was devised for binary classification or classifying data into two types and extended for multi-classification.

2.2.1: Binary and multi Classification

Binary classification, as the name suggests, means classifying data into two categories. We are provided with some data points, or training patterns. We know for each of them, whether the pattern belongs to the first category or the second. Next, we are presented with some more data points but we do not know their respective classes. These new data points are called test patterns.The optimal separating hyperplaneseparates the two classes and maximize the distance to the closest point from either class. This provides a unique solution to the separating hyperplane problem. By maximizing the margin between the classes, it leads to better classification.

2.2.2: Linear and nonlinear classification

In binary and multi-classification it can be a linear or nonlinear classification depending upon the type of data. For the classification of the data classifiers are formulated for classification. There are kernel function which helps in the classification of the data. Kernel function transforms the data from lower dimensional space to higher dimensional space making the data more visible and predictable. We have different type of kernel functions which can be used accordingly. Figure 2.1 shows the linear and nonlinear situations for classifications. Separate kernels are used for classifying both the cases[5].

(A)   (B)
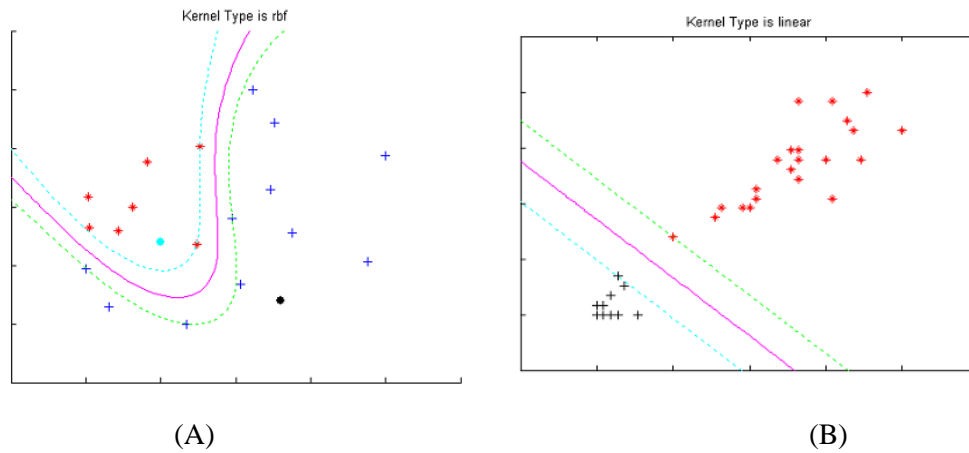
Figure 2.1 : (A) Nonlinear Classification using radial basis Kernel function, (B) Classification using Linear Kernel.

2.2.3: Kernel Machine

The original optimal hyper plane algorithm proposed by *Vapnik* in 1963 was a linearclassifier. However, in 1992, *Bernhard E. Boser, Isabelle M. Guyon and Vladimir N. Vapnik*[6] suggested a way to create nonlinear classifiers by applying the kernel trick(originally proposed by Aizerman et al. to maximum-margin hyper planes. The resulting algorithm is formally similar, except that every dot product is replaced by a nonlinear kernel function. This allows the algorithm to fit the maximum-margin hyper plane in a transformed feature space. The transformation may be nonlinear and the transformed space high dimensional; thus though the

classifier is a hyper plane in the high-dimensional feature space, it may be nonlinear in the original input space.

Some common kernels include:

- Polynomial (homogeneous): $k(x_i, x_j) = (x_i, x_j)^d$
- Polynomial (inhomogeneous): $k(x_i, x_j) = (x_i, x_j + 1)d$
- Gaussian radial basis function: $k(x_i, x_j) = exp(-\sqrt{} || x_i - x_j||2)$, for $\vee > 0$. Sometimes parameterized using $\sqrt{} = 1/2\sigma2$
- Hyperbolic tangent: $k(x_i, x_j) = tanh(kx_i, x_j + c)$, for some (not every) $k > 0$ and $c < 0$,

The kernel is related to the transform $\Psi(x_i)$ by the equation $k(x_i, x_j) = \Psi(x_i). \Psi(x_j)$.

2.2.4: Formulation of the Quadratic Programme for the SVM

We will derive the solution for the optimal canonical separating hyperplane when the data are linearly separable. We note that this hyperplane is a canonical separating hyperplane with the maximal margin.

The margin
$$M = (x_1 - x_2) w$$

Here the subscript w denotes the projection of the vectors x_1 and x_2 onto the weights vector direction. Taking projections along w, we get
$$D_1 = || x_1 || \cos(\alpha),$$
$$D_2 = || x_2 || \cos(\beta),$$
$$M = D_1 - D_2,$$

Where α and β are the angles between w and x_1 and w and x_2 respectively. We know that

$$\cos(\alpha) = [x_1^T w / ||x_1|| * ||w||]$$

$$cos \ (\beta) \ = \ [\ x_2^T \ w \ / \ ||x_2|| \ * \ ||w|| \ ]$$

Substituting, this leads to

$$M \ = \ (x_1^T - \ x_2^T) \ w \ / \ ||w||$$

And x_1, x_2 are the support vectors satisfying

$$Y_j \ = \ | \ w^T x_j \ + \ b \ | \ = \ 1, j \ = \ 1,2$$

We have

$$w^T x_1 \ + \ b \ = \ 1, w^T x_2 \ + \ b \ = \ -1$$

And finally we get

$$M \ = \ 2 / \ || \ w \ ||. \hspace{4cm} 2.11$$

We could also get this result using the fact that the distance D between a support vector x_1 and a canonical separating line is equal to half the margin M and therefore

$$D \ = \ M \ / \ 2 \ = \ | \ w^T x_2 \ + \ b \ | \ / \ || \ w \ || \ = \ 1 \ / \ || \ w \ ||,$$

from where

$$M \ = \ 2 / \ || \ w \ ||,$$

as before.

Therefore to maximize the margin M, we need to minimize

$$|| \ w. \ ||. = \ (\ w_1^2 \ + \ w_2^2 \ + \cdots ... + \ w_n^2 \ )^{1/2} \hspace{3cm} 2.12$$

The optimal canonical separating hyperplane with the maximal margin will specify support vectors that are the training points closest to the Optimal Canonical Separating Hyperplane (OCSH) by where N_{SV} denotes the total number of support vectors. At the same time, all training points must satisfy the following inequalities.

$$Y_j \;=\; |\,w^T x_j + b\,| \;=\; 1, \, j = 1\ldots l \tag{2.13}$$

Thus to find the optimal separating hyperplane with the maximal margin, we need to minimize $\|w\|$, which is the same as minimizing $\|w\|^2$. You will recognize that this is a standard non-linear optimization problem with inequality constraints, which can be solved by the method of Lagrange multipliers.

Let

$$L\,(\,w,b,\alpha\,) \;=\; \tfrac{1}{2}\, w^T w \;-\; \sum \alpha_i \{ y_j [w^T x_j + b] - 1 \} (\text{for } i = 1 \text{ to } l) \tag{2.14}$$

where the α_i's are the Lagrange multipliers. The Lagrangian L is to be minimized with respect to wand band maximized with respect to the non-negative α_i's. Instead of solving the problem in the primal space (the space of w and b) it is more insightful to solve the problem in the dual space (the space of the α_i's). Applying the Karush-Kuhn-Tucker conditions, at the optimal solution (w0, b_0 , α_0) the derivatives of the Lagrangianwith respect to the primal variables will vanish, so that

$$\partial L \,/\, \partial w_0 \;=\; 0, \, or \; w_0 \;=\; \sum \alpha_i y_i x_i \quad (\text{for } i = 1 \text{ to } l) \tag{2.15}$$

$$\partial L \,/\, \partial b_0 \;=\; 0, \, or \sum \alpha_i y_i \;=\; 0 \quad (\text{for } i = 1 \text{ to } l) \tag{2.16}$$

Applying the complementary conditions we have

$$\alpha_i \, \{ y_i [\, w^T x_j + b \,] - 1 \} \;=\; 0, \quad i = 1 \ldots l \tag{2.17}$$

Using equations further

$$L_d\,(\alpha) \;=\; \sum \alpha_i \;-\; \tfrac{1}{2} \sum \alpha_i \alpha_j y_i y_j x_i^T x_j \tag{2.18}$$

We need to maximize the dual Lagrangian$L_d(\alpha)$ with respect to the non-negative α_i's

$$\alpha_i \;>\; 0, \, i = 1 \ldots l$$

24

The dual Lagrangian$L_d(\alpha)$ is expressed only in terms of the training data, and it depends on the scalar product of the input training patterns $- x_ix_j$. This is very important because we will see that instead of using x_ix_j we will be able to use other types of inner products.

Our formulation is a standard Quadratic Programming problem. We can put this in matrix notation.

Maximize $\qquad\qquad\qquad\qquad L_d\,(\alpha)\; =\; -0.5\,\alpha^T\,H\alpha\; +\; f^{\,T}\alpha$ $\qquad\qquad\qquad$ 2.19

Subject to

$$y^T\alpha\; =\; 0,$$
$$\alpha\; >=\; 0$$

where H denotes the Hessian matrix $H_{ij}\; =\; y_iy_jx_ix_j\; or\; y_iy_jx_i^T\,x_i$ and f = 1 is a unit vector.

After we find out the solution $\alpha_0$of the QP, we can find the parameters $w_0$and b, as follows

$$w_0\; =\; \Sigma\,\alpha_i y_i x_i, \text{i} = 1\ldots l \qquad\qquad\qquad 2.20$$
$$b_0\; =\; (\,1\,/\,N_{SV}\,)\,[\,\Sigma\,\{\,(\,1\,/\,yS\,) - xS^T w_0\}\,]\,,S\; =\; 1\ldots N_{SV}$$

when using a kernel function K, we will replace $x_i^Tx_j$ by K (x_ix_j) $= \Phi^T($ x_i) $\Phi($ x_j)and subsequently.

Chapter3
Two Phase Flow through Pipe

In this chapter two phase flow through a pipe is explained, and information about all the flow regimes with their characteristics is provided. All the correlations, which are used for the generation of data,along with the development of LDA and SVM classifiers are presented here.

3.1 Flow Patterns in Two-Phase Flow

Simultaneous flow of several fluids with different fluid flow properties is more complex than single-phase flow[6]. The influence of one phase over the other permits a flow regime (i.e., a specific distribution of each phase in the pipe relative to the other phase) to develop. Such apattern may become unstable when the flow conditions change, consequently transitioning to another pattern,which at some point can also become unstable. Bychanging the flow rates of the gas and the liquid, thistransition from one pattern to another can go on untilall possible flow regimes can be observed. Some of theconventionally identified flow regimes are as followsannular flows, bubble flows, churn flows, stratifiedsmooth flows, stratified wavy flows, and dispersedbubble flows.

3.1.1: Vertical Flow. The vertical upward flow has four primary flow patterns, as accepted by most researchers[7].Their characteristics are described below.

3.1.1.1: Bubble Flow: In the bubble flow regime, the uniformly distributed gas phase flows as discrete bubbles in a continuous liquid phase. Bubble flow can be further divided into two types of flow, bubbly and dispersed bubble (DB) flow. In bubbly flow, the presence of slippage in the bubble flow allows relatively fewer and larger bubbles to move faster than the liquid phase, while in DB, numerous small bubbles are transported by the liquid phase due to the absence of slippage in the bubble flow, causing no relative motion between the two phases.

3.1.1.2: Slug Flow: In slug flow (which appears upon increasing the gas flow rate in bubble flow), the bubble concentration becomes high, coalescence occurs, and the largest bubbles are of the same cross-section as that of the pipe. Slug flow is characterized by a series of slug units composed of bullet-shaped gas pockets called gas

plugs or Taylor bubbles, plugs of liquid called slugs, and a film of liquid around the Taylor bubble flowing vertically downward (there are also some gas bubbles distributed throughout the liquid). The liquid slugs carrying the gas bubbles bridge the pipe and separate two consecutive Taylor bubbles.

3.1.1.3: Churn Flow: Churn flow is a highly disorganized flow of a gas-liquid mixture, in which the vertical motion of the liquid is oscillatory and alternating. There are similarities with slug flow in that both phases do not exhibit any dominance over the other, i.e., neither phase appears to be continuous. The difference from slug flow is that the gas plugs become narrowerand more irregular; the continuity of the liquid in the slugs is repeatedly destroyed by regions of high gas concentration, and the thin film of liquid surrounding the gas plugs is absent. Both slug and churn flow can be considered intermittent flow. Some researchers also define a sub region of the churn flow as froth flow, 15 which occur at higher gas velocities and exhibit a frothy mixture consisting of large bubbles.

3.1.1.4: Annular Flow: In annular flow, gas flowsalong the center of the pipe. The liquid flows upward, both as film and as dispersed droplets in the gas core. At high gas velocities, liquid becomes dispersed in the gas core, leaving a very thin film of liquid flowing along the pipe wall. Vertical flow pattern maps are used to predict the flow pattern in a vertical upward pipe that will occur for a given set of parameters, namely, flow rates, fluidproperties, and pipe diameter. *Taitel et al.* **[8]** developed a theoretical model for gas-liquid flows in vertical tubes. They identified the four distinct flow patterns mentioned above: bubble, slug, churn, and annular flow. They studied the physical mechanisms, taking into account the influence of fluid properties, pipe size, and flow rates by which regime transitions occur, and developed models for transition criteria. Weisman and Kangusing experimental data, pro-posed a theoretical model for vertical and upwardly inclined lines, with the exception of the vertical bubble-intermittent transition, which the authors contended can be described as the relationship between the gas phase and the total Froude number. The model also incorporated the effect of fluid properties and pipe diameters. They concluded that the behavior pattern is consistent with

that seen in horizontal lines for the 2.5 cm and above pipes, both for the dispersed and annular transitions. *McQuillan and Whalley* **[9]** developed a theoretical approach for flow patterns in vertical two-phase flow. A correlation was developed for the plug flow-churn flow transition based on the assumption that the gas flow rate in the plugs increases until it causes the flooding of the falling liquid film around the plug. Modifications were also made on the analysis for determining the stability of bubble flow and annular flow, respectively. *Miet al.* **[10]**developed a neural network (NN) model for vertical flow regime identification from the impedance signal of laboratory instruments during a two-phase flow experiment. The NN model was based on two-phase flow models, such as the drift-flux model and a slug-flow model, and a two-phase flow experimental database to obtain the impedance used as the input data for training and testing of the NN model. It have beenchosen the impedance as input to the NN model. Impedance signals were measured by an impedance void meter. In our work, we adopted the superficial phase velocities and the pipe diameter as inputs for the MSVM model, instead of using the impedance as a model input, to develop a generally useful tool that can be used when a database already exists.

3.1.2: Horizontal Flow: Horizontal flow patterns are more complex than vertical flows due to gravitational forces. Gravity causes an asymmetric distribution of the phases by forcing the liquid phase to progress toward the bottom of the pipe. Described briefly below are the main patterns of horizontal flow that are widely accepted.

3.1.2.1: Stratified Smooth Flow (SS): For the SS flow, the gravitational separation of the liquid and gas phase is complete. Liquid flows at the bottom of the pipe, and gas flows at the top.

3.1.2.2: Stratified Wavy Flow (SW): At increasing gas velocity in the SS flow, large waves start to develop on the liquid stratum giving the Stratified Wavy flow regime. Both SS and SW can be considered stratified flows.

3.1.2.3: Slug Flow: At increasing gas velocity in the SW flows, the waves of the liquid phase become largeenough to reach the upper surface of the pipe. The liquidwets the whole pipe surface, allowing liquid film to cover the surface between the bridging waves or slugs.

3.1.2.4: Plug Flow: This is similar to the verticalupward slug flow, with bullet-shaped bubbles that tend to move along in a position closer to the top of the pipe. The liquid layer separating the gas bubble from the wall also tends to be thicker at the bottom of the pipe than at the top. Both slug and plug flows can be considered as intermittent flows. Also part of intermittent flows is the elongated bubble flow, which is considered a limiting case of slug flow free of entrained gas bubbles.

3.1.2.5: Dispersed Bubble Flow (DB): Such flow occurs at high liquid rates and low gas rates. The gas phase is distributed as discrete bubbles within a continuous liquid phase. It can be characterized as a pipefull with a liquid that has small bubbles dispersed uniformly throughout.

3.1.2.6: Annular Flow: This is similar to the vertical annular flow, which occurs at higher gas velocities, except that the liquid is much thicker at the bottom of the pipe than at the top. Horizontal flow pattern maps are used to predict the flow pattern in a horizontal pipe that will occur for a given set of parameters, namely, flow rates, fluid properties, and pipe diameter. A theoretical approach is proposed, perhaps the most significant contribution to the prediction of flow patterns in horizontal and near-horizontal gas-liquid flow. The regimes identified were: dispersed bubble, intermittent, stratified smooth and wavy, and annular flow. They showed that transitions between flow regimes were controlled by the fluid properties and the pipe size and can be represented by a set of two dimensionless groups. The test cases for flow pattern covered a wide range of fluid properties in pipes varying in diameter from 1.2 to 5 cm. Comparisons were made with available literature data, and a revised dimensionless correlation was presented. *Osman and Ternyik et al.* **[9]** developed a NN model for horizontal flows using the gas and liquid fluid properties and flow rates, the liquid holdup, the pressure, the pipe

diameter, and the temperature as inputs into the NN model. The output was a horizontal flow regime map. The NN models were successful, reporting better predictions and higher accuracy than the empirical correlations for the group of data used.

3.2 Correlations for Flow regimes

3.2.1 Vertical Flow: The transition equations for the data generation used for the prediction of the vertical flow regimes map were based on the work of *McQuillan and Whalley* **[9]** and are as follows.

Bubble-intermittent flow transition

$$V_{LS} = 3.0 * V_{GS}^{-1.15}[\,g\,\sigma\,(\,\rho_L - \rho_G\,)\,/\,\rho_L{}^2\,]^{1/4} \qquad\qquad 3.1$$

Bubble-dispersed bubble flow transition

$$V_{LS} >= (6.8\,/\,\rho_L{}^{0.444}) * \{\,g\,\sigma\,(\,\rho_L - \rho_G\,)\,\}^{0.278}(\,D/\,\mu_L\,)^{0.112} \quad 3.2$$

Transition to annular flow

$$V_{GS} >= [\,\{\,g\,D\,(\,\rho_L - \rho_G\,)\,\}\,/\,\rho_G]^{1/2} \qquad\qquad 3.3$$

3.2.2 Horizontal Flow: Horizontal flow patterns aremore complex than vertical flows due to gravitationalforces. Gravity causes an asymmetric distribution of thephases by forcing the liquid phase to progress towardthe bottom of the pipe.

The transition equations for the data generation used for the prediction of the horizontal flow map were based on the work of *Weiseman***[8].**

Stratified-intermittent transition

$$V_{GS} / (g\,D)^{1/2} = 0.25 * (V_{GS}/V_{LS})^{1.1} \qquad 3.4$$

Stratified wavy-stratified smooth transition

$$(\sigma/g\,D^2\,\Delta\rho)^{0.20} (D\,G/\mu_G)^{0.45} = 8 * (V_{GS}/V_{LS})^{0.16} \qquad 3.5$$

$$\Delta\rho = \rho_L - \rho_G$$

Transition to annular flow

$$1.9 * (V_{GS}/V_{LS})^{1/8} = Ku^{0.2}Fr^{0.18}$$

$$= (V_{GS}\rho_L [g\,(\rho_L - \rho_G)\,\sigma]^{1/4})^{0.2} * (V_{GS}^2/g\,D)^{0.18} \qquad 3.6$$

3.3 Result and discussion

3.3.1: Classification using LDA Technique

Figure 3.1 shows the classification of the flow regimes using Linear Discriminant Analysis

Figure 3.1: (A) Multi-Classification [all three regimes are separated together] (B) Binary Classification Intermittent and Annular Flow Regimes (C) Binary Classification Intermittent and

Bubble Dispersed Flow Regimes (D) Binary Classification Bubble Dispersed and Annular Flow Regimes.

3.3.2: Classification using SVM Technique

Figure 3.2 shows the classification of the flow regimes using Support Vector Machine.
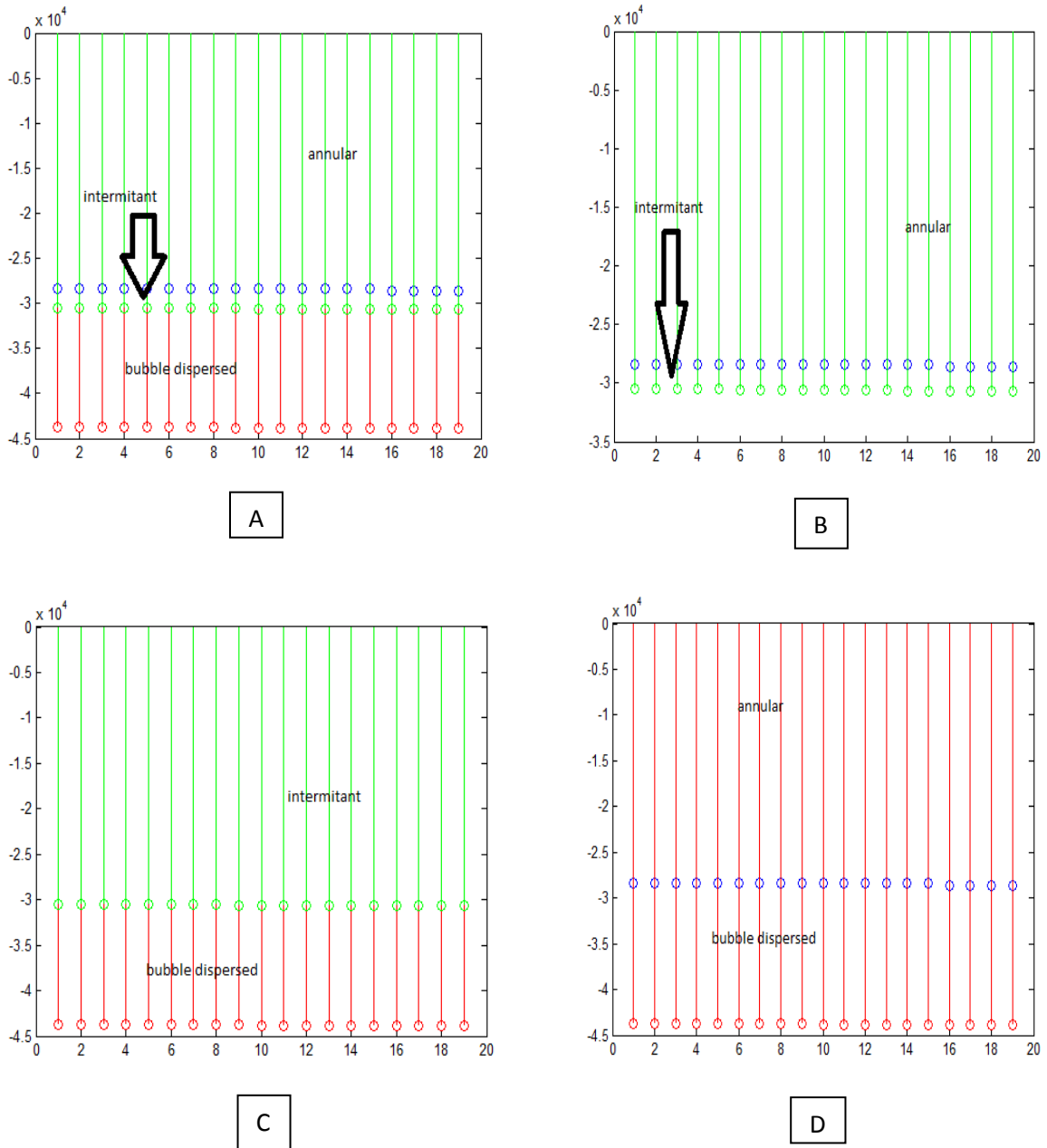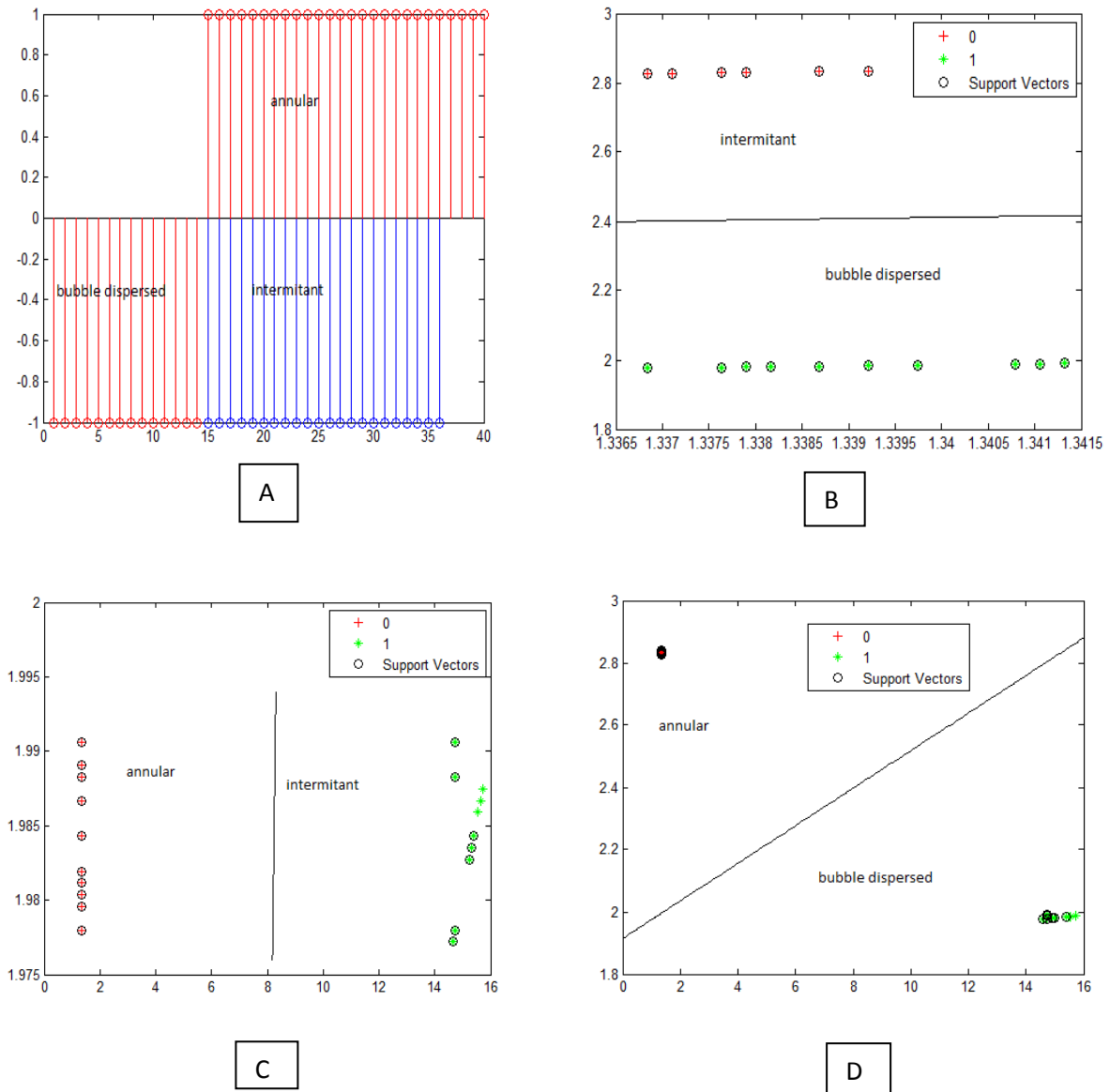

Figure 3.2: *(A) Multi-Classification [all three regimes are separated together] (B) Binary Classification Intermittent and Bubble Dispersed Flow Regimes (C) Binary Classification*

Intermittent and Annular Flow Regimes (D) Binary Classification Bubble Dispersed and Annular Flow Regimes.
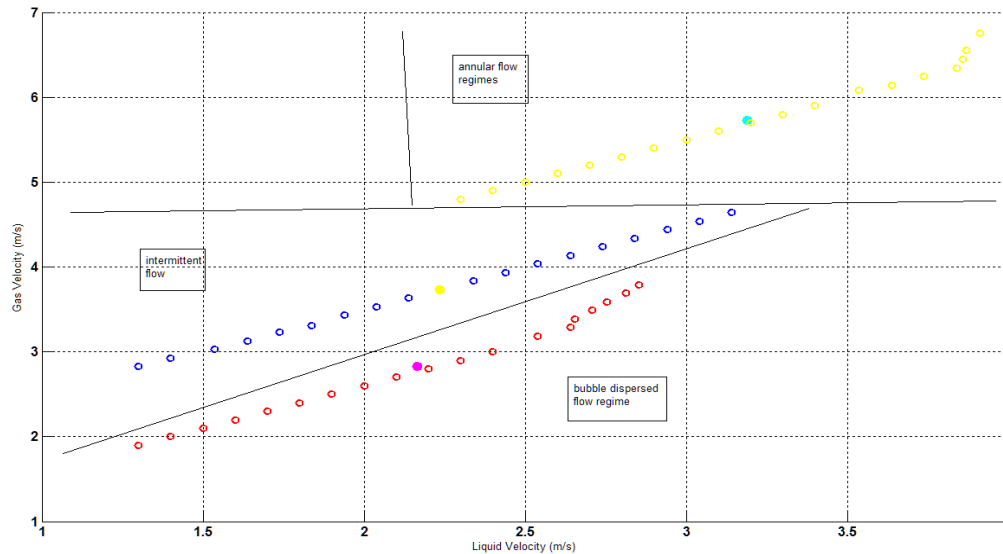
Figure 3.3: *Multi-classification of all regimes together using LDA*

We used literature based data for the analysis. Correlations provided in research papers of various scientists and researchers are used for generating the data for the study. The data sets for different flow regimes which are provided in the appendix C. For different flow regimes of flow through a pipe, classification is done. Binary and multi classification of the data is done by using both the techniques Linear Discriminant Analysis and Support Vector Machine. The data is classified and visible and predictable by using these techniques.

In Figure 3.1 LDA classification is done and stem plot is drawn. Figure 3.1 - A shows the classification of all the flow regimes together and each class is represented with different color circle. Similarly Figure 3.1 - B, C, D represents the binary classification by taking two classes together only. In Figure 3.2– Aplot is made forthe classification of all the regimes together but by using different technique SVM.And Figure 3.2 B, C, D shows the plots for binary classification of flow regimes.

We used two functions for plotting the data namely as *plot* and *stem* function. For understanding *plot*(y) plots the values in vector y versus their index. *plot*(x,y) plots the values in vector y versus x. plot produces a piecewise linear graph between its data values. With enough data points it looks continuous. Using *stem*(y) the data sequence y is plotted as stems from the x axis terminated with circles for the data values. *stem* is the natural way of plotting sequences.

stem(x,y) plots the data sequence y at the values specified in x.*stem*(Y) plots the data sequence, Y, as stems that extend from a baseline along the *x*-axis.

In figure 3.3 classification of all the regimes together is done using LDA and on the basis of the axial parameters regimes are drawn.

Mat Lab Instructions are provided for this formulation in ***Appendix B.*** We used polynomial classifiers for multi-classification of data. Classifiers are also provided in ***Appendix B.***

Data was generated using appropriate correlations provided. Complete data sets are provided in the ***Appendix C***, a sample calculation for generation of data is also mentioned in the appendix..

Chapter 4
Flow through Two Phase Inverse Fluidized Bed

4.1: Flowthrough Inverse fluidized bed

Inverse fluidization is a technique in which solid particles having lower density than that of the liquid, are kept in suspension by the downward flow of continuous liquid phase. In three phase system, gas is introduced countercurrently to the liquid flow [9]. This chapter provides the literature about different fluidized bed regimes in two-phase Inverse fluidized bed. All the correlation corresponding to each fluidized bed regime is provided.Finally the development of LDA and SVM based classifier designs are provided.

4.2: Literature and Correlations for Fluidized Bed regimes

Liquid-Solid Circulating Fluidized Beds (LSCFBs) are gaining in popularity for their wide range of potential applications because of their many advantages including significantly high mass and heat transfer rates, improved liquid-solid contact efficiency, easy control of large quantity of particles etc. The design, scale up and operation of such liquid-solid continuous systems require information of phase holdup and flow patterns referred to as the hydrodynamic characteristics.

Fluidised bed reactors have proved their versatility for carrying out aerobic fermentation process, catalytic reaction and biological treatment of waste water. Fluidisationwhere the liquid is a continuous phase is commonly conducted with an upward flow of liquid in liquid-solid systems or with an upward co-current flow of gas and liquid in a gas-liquid-solid system. Under these fluidising conditions the solid particles has a density greater than that of liquid. When the density of solid particles are less than the continuous liquid phase then fluidisation can be achieved by a downward flow of liquid to counter net buoyancy force of the particles. Such type of fluidisation is termed as inverse fluidisation. The inverse fluidised bed reactor (IFBR) is a very efficient system for the biological treatment of waste watersystem when compared to an up-flow fluidised bed reactor because in an inverse fluidised bed reactor, the control of biofilm thickness is achieved within a very narrow range.The inverse fluidised bed reactor is also used in ferrous iron oxidation by Thiobacillus ferro-oxidants and for the hydrolysis of milk protein.

Furthermore, an object with a higher density than the bed will sink, whereas an object with a lower density than the bed will float, thus the bed can be considered to exhibit the fluid behaviour expected of Archimedes' principle. As the "density", (actually the solid volume fraction of the suspension), of the bed can be altered by changing the fluid fraction, objects with different densities comparative to the bed can, by altering either the fluid or solid fraction, be caused to sink or float.

In fluidized beds, the contact of the solid particles with the fluidization medium (a gas or a liquid) is greatly enhanced when compared to packed beds. This behaviour in fluidized combustion beds enables good thermal transport inside the system and good heat transfer between the bed and its container. Similarly to the good heat transfer, which enables thermal uniformity analogous to that of a well-mixed gas, the bed can have a significant heat-capacity whilst maintaining a homogeneous temperature field.

In the reference of the study a lot of work has been done in this research area. *R.J. FeminBendict, G. Kumaresan, M. Velan* **[11]** did the study regarding the bed expansion and pressure drop by varying the flow rate. A perfect situation was determined in the study for a specified operation which really corresponds to a specific fluidized bed situation. And simply it can be understand that considering the aspect of best heat transfer and mass transfer the specification for fluidized bed is required. In one more doctorate thesis by *Long Sang* **[12]** importance of this specification and classification can be seen.

In the same aspect we have classified the fluidized bed situation, and obviously as clear from the referred studies that for a specified fluidized bed situation pressure drop and velocities are considerable and they have a specified range as well. On the basis of these parameters we have classified the fluidized bed regimes. In our study we have taken the particles having the density lower than that of the liquid.

Correlations are proposed for pressure drop in the packed bed regime, for bed expansion in the semi fluidized bed regime and in the fully fluidized bed regime, for onset ofsemi fluidization and for the minimum fluidization of the complete bed of solids. All these correlations are used to predict the overall bed pressure drop in the whole range of operation **[10].**

4.2.1: Packed bed regime

The friction factor correlation obtained is as follows:

$$f = 60\, R_{em}^{-0.415}\, ,\ 325 < R_{em} < 5760 \tag{4.1}$$

Where the friction factor is defined as

$$f = (\Delta P)p\, dp\epsilon_p^3 / [\, (\rho\, U_1^2)\, HP\, (1 - \epsilon_p)] \tag{4.2}$$

4.2.2: Semi fluidization regime

$$U_{osf} = (5.6 * 10^{-2}) * Ar^{0.0064} * [\, (\rho - \rho_s) / \rho\,]^{0.52} \tag{4.3}$$

$$10^6 < A_r < 7*10^7,\ 0.4 < (\rho-\rho_{s}/\rho) < 0.9$$

Height for the correlations

$$\left(\frac{H_f}{H_c}\right) sf = 4.6 * Ar^{-0.19}[\, (\rho - \rho_s) / \rho]^{-1} \tag{4.4}$$

$$(\frac{H}{H_0}) sf = 0.7\, R_e^{0.4} Ar^{-0.14}\, [(\rho - \rho_s)/\rho]^{0.1} \tag{4.5}$$

$$10^6 < A_r < 7*10^7 \quad 0.4 < (\rho-\rho_{s}/\rho) < 0.9 \quad 512 < R_e < 2040$$

4.2.3: Fully fluidized bed regime

$$U_{ms} = 2.93 * 10^{-4} * Ar^{0.202} * [(\rho - \rho_s)/\rho]^{0.38} \tag{4.6}$$

$$10^6 < A_r < 7*10^7\, ,\ 0.4 < (\rho-\rho_{s}/\rho) < 0.9$$

The pressure drop due to fluidized solids can be estimated from the equation

$$(\Delta P)_f \; = \; (\,1 - \,\epsilon\,)\,(\,\rho - \rho_s\,)\,g\,H_f \qquad\qquad 4.7$$

Where

$$\epsilon_f \; = \; 1 - [(Ho - Hp)\,/H_f]\,(1 - \epsilon_p) \qquad\qquad 4.8$$

We generated the data by using these correlations. Data sets with sample calculation for fluidized bed regimes are provided in **Appendix D**.

4.3: Result and discussion

4.3.1: Classification using LDA Technique

Figure 4.1 shows the classification of Fluidized Bed regimes using Linear Discriminant Analysis.

A

B

41
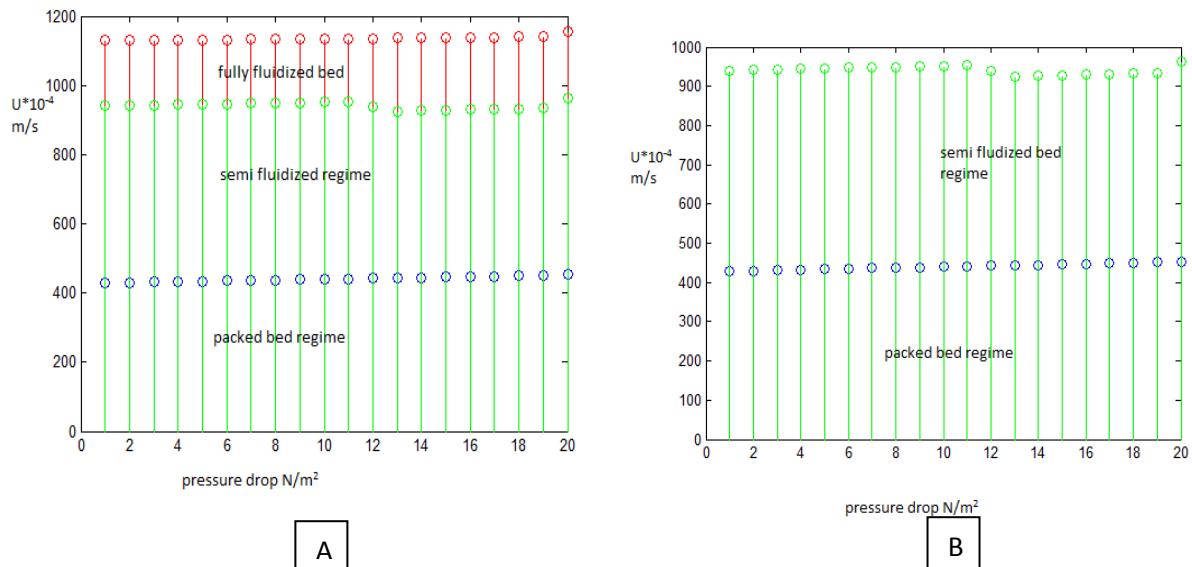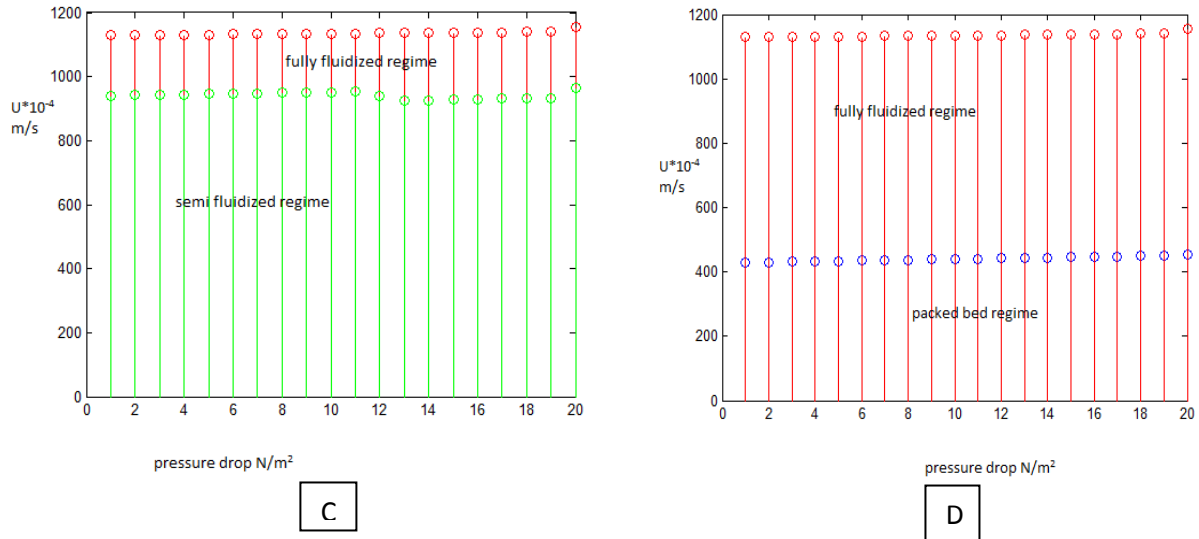
Figure 4.1: (A) Multi-classification [classification of all fluidized bed regimes together], (B) classification of Semi Fluidized and Packed Bed regime, (C) classification of Semi Fluidized and Fully Fluidized regimes, (D) classification of Fully Fluidized and Packed Bed regime.

4.4.2: Classification using SVM Technique

Figure 4.2 shows the classification of the fluidized Bed regimes using Support Vector Machine Technique.

C

D
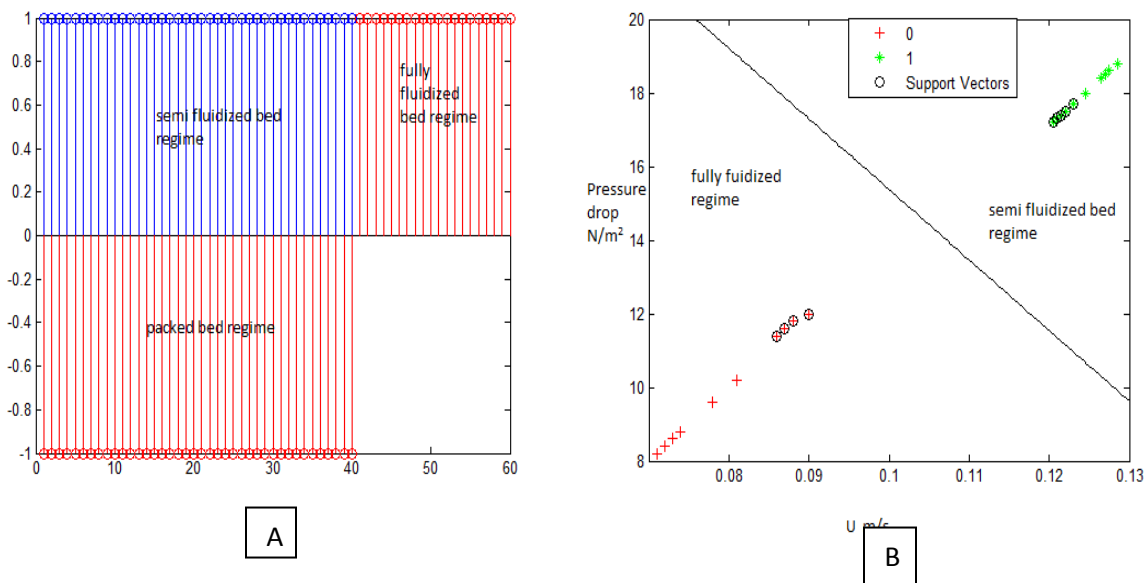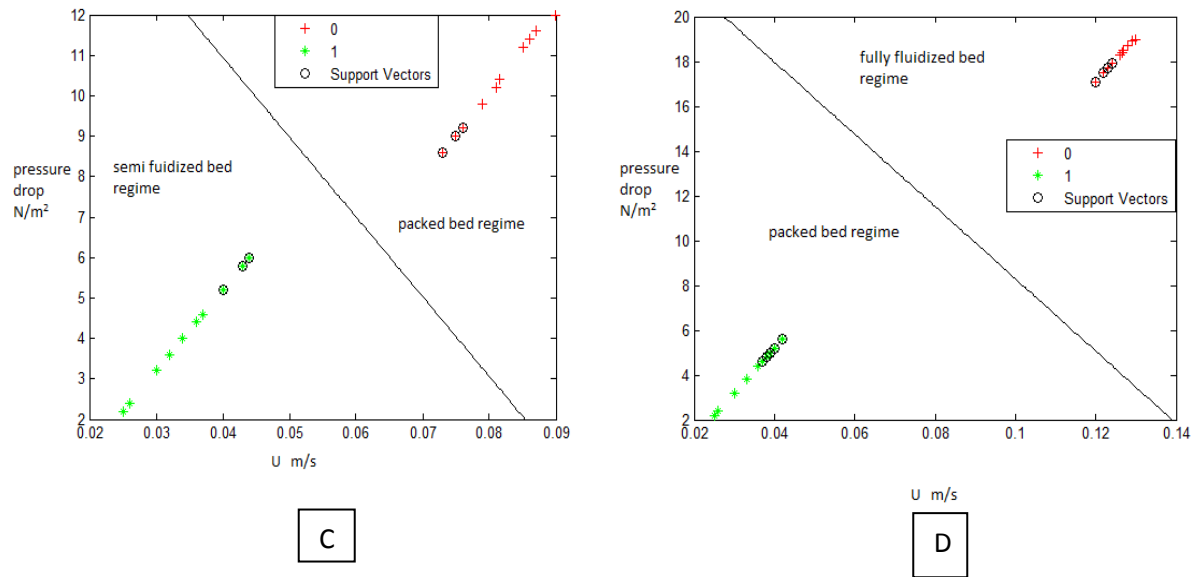
Figure 4.2: (A) Multi-classification [classification of all the fluidized bed regimes together], (B) classification of Semi Fluidized and fully fluidized Bed regime, (C) classification of Semi Fluidized and Packed Bed regime, (D) classification of Fully Fluidized and Packed Bed regime.
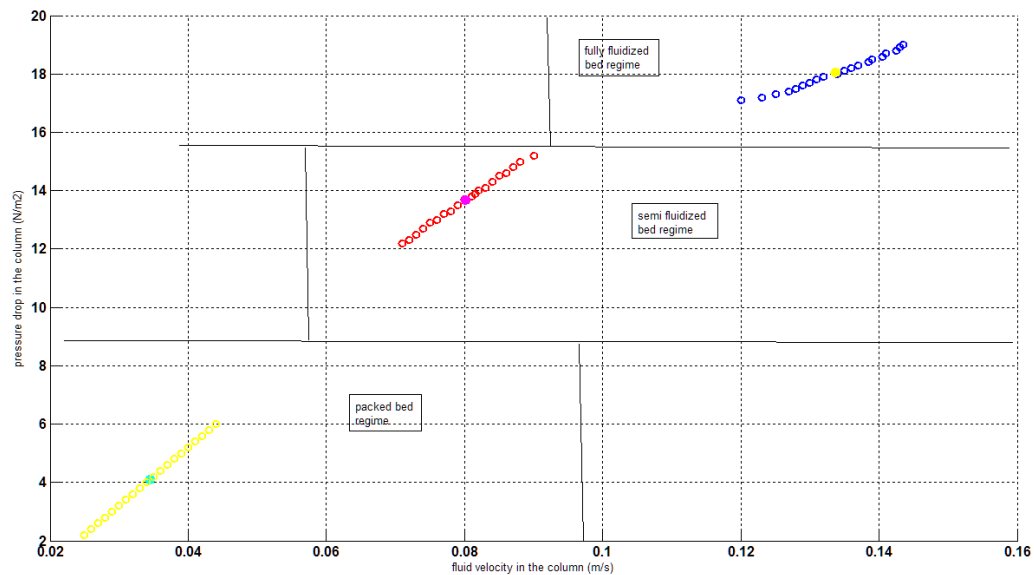
Figure 4.3: *Multi-classification of all fluidized bed regimes using LDA*

For different fluidized bed regimes while Two Phase Inverse Fluidization, classification is done. Binary and multi classification of the data is done by using both the techniques Linear

Discriminant Analysis and Support Vector Machine. The data is classified and visible and predictable by using these techniques.

In Figure 4.1 LDA classification is done and stem plot is drawn. Figure 4.1 - A shows the classification of all the packed regimes together and each class is represented with different color circle(supportvectors). Similarly Figure 4 - B, C, D represents the binary classification by taking two classes together only. In Figure 4.2 - A plot is made for the classification of all the packed bed regimes together but by using different technique SVM. And Figure 4.2 B, C, D shows the plots for binary classification of flow regimes using SVM. In Figure 4.3 classification of all the regimes is done using LDA. Scattered data in Figure 4.3 can be seen in the result plot in their respective regimes. Regimes are drawn by taking the axial parameters in the consideration.

Chapter 5
Effect of diameter and density variation on fluidization in gas fluidized bed

5.1: Effect of variation in the diameter and density of fluidization particles in Geldart B Fluidization regime

In chemical engineering operations gas fluidization has its own importance as it is used in many processes where the perfect quality of fluidization is required. In the study it is shown that for a particular fluidization we can use a range of different materials and required fluidization is achieved. We showed in the study that though different materials can be used for a specified fluidization regime but there is an appreciable effect of changing the density and diameter of the fluidization particle.*George D. Cody, JayatiJohri, David Goldfarb*[13] did a study showing the effect of diameter and desity variation of particles. They concludes that a great effect in the characteristic velocities of fluidization can be seen.So this observation is also important to have the appropriate operation. We have taken the particles of Geldart B and A fluidization for the study. The materials which we have used are Glass, Nickel, ASN Polymer.

The data table for the particles is

Table 1: data for different Geldart B and A fluidization particles.

Measurement	ρ_p g/cm^3	μ_f $\mu poise$	D μm	D_b^0 μm	U_{mf}^* cm/s	$\emptyset_{mf}$	n
ASN Glass R87	2.45	210	149	128	1.6	0.613	4.718
ASN Glass R63	2.45	210	210	121	3.7	0.597	4.765
ASN Polymer 1	1.04	210	320	174	3.5	0.601	4.735
ASN Polymer 2	1.04	210	650	178	10.0	0.640	4.639
ASN Nickel	8.9	181	76	44.8	4.27	0.511	5.025

Five different types of particles having different densities and diameters are used. All the properties of the particles are mentioned in the table 1 (appendix E).

For the generation of the data, the following correlations are used from literature **[13]**.

The semi-empirical Ergun Equation, defines the minimum fluidization velocity, for low Reynolds numbers, as the superficial gas velocity at which the viscous pressure drop across the fixed bed is equal to the weight of the bed,

$$U_{mf}^* = [\frac{(1 - \emptyset_{mf})^3}{150 \, \emptyset_{mf}}](\frac{D^2 \rho_p g}{\mu_f})$$

for later convenience, we have introduced the Stokes velocity,

$$U_t = [\frac{D^2 \rho_p g}{18 \mu_f}]$$

The sphere concentration $\emptyset_{mf}$, at U_{mf}^* is the only free parameter.

The correlation used for the calculation of superficial gas velocity is widely used *Richardson Zaki equation*.

$$U_s = (1 - \emptyset)^n U^t$$

The data generated is mentioned in the ***Appendix E.***

5.2: Classification Using LDA (Diameter and Density Variation)

Furthermore the classification of the data is done when it was having the distinction because of the density and diameter variation. Figure 5.1 shows the results of the study which clearly shows the classification for particles having diameter and density variation.
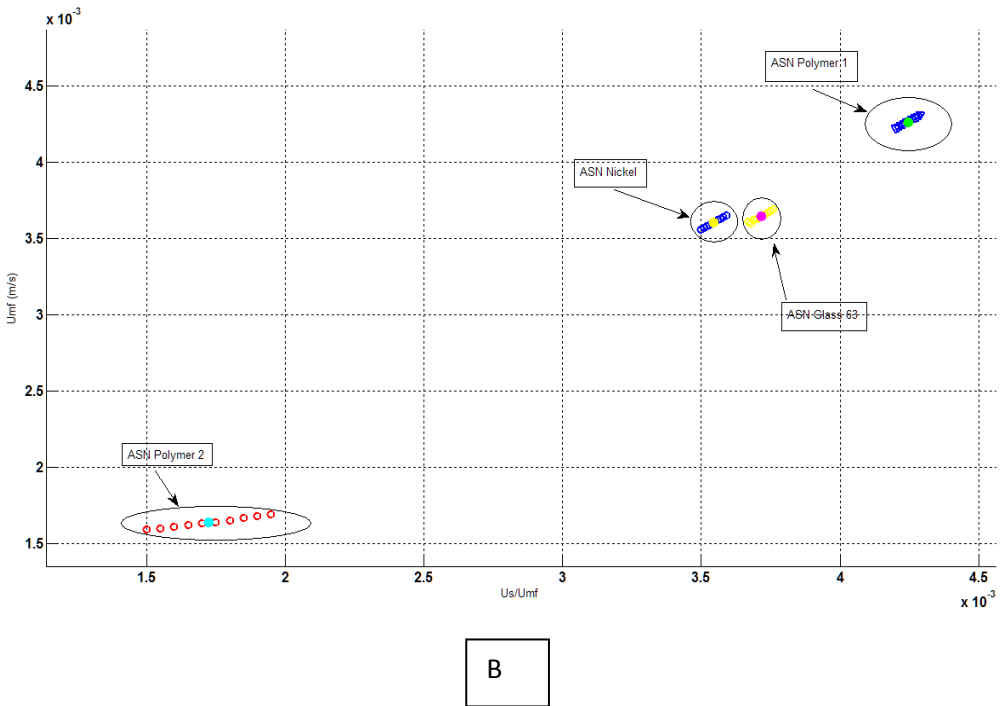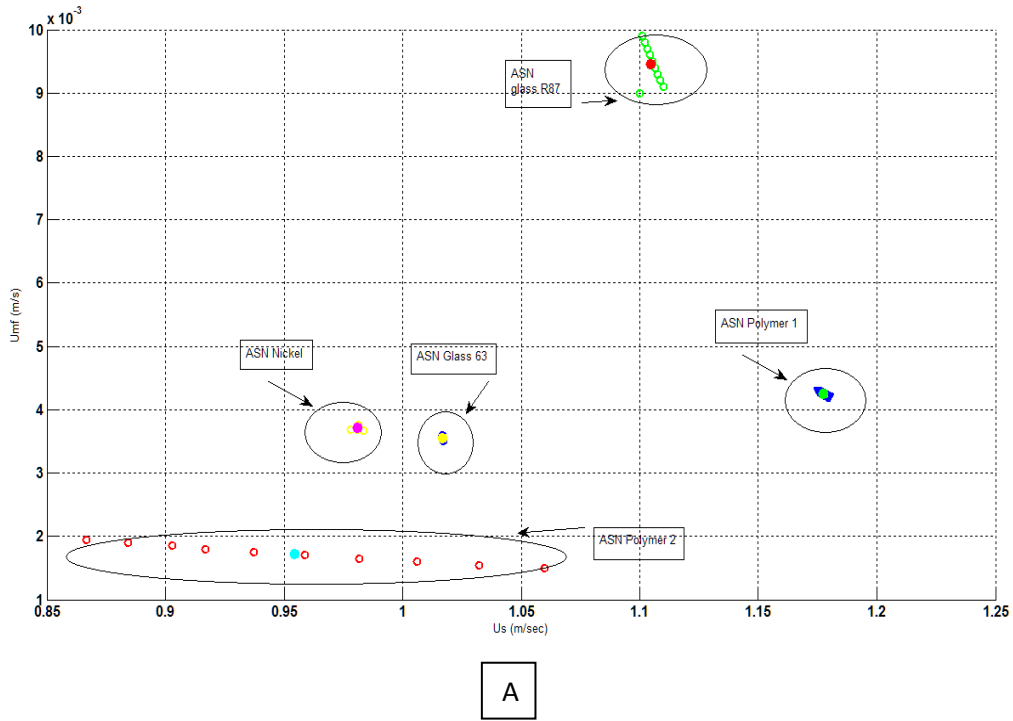
Figure 5.1: *Figure 5.1 A,B shows the classification of the data generated for the particles of different diameter and density.*

Figure 5.1 shows the fluctuation velocity variations in the onset fluidization velocity and gas superficial velocity by using particles of different diameter and density. Basically study tells that all the particles used in this study are appropriate for the operation in Geldart B regime (which has its own fluidization properties), but still they can affect the quality of the fluidization. In the figure we can see that how the velocity relation variations are taking place thought all the particles fall in Geldart B and A fluidization. In figure B also variation is classified using another fluidization parameter. So we really need to select the appropriate particles for desired fluidization and requirements, and by this study it can be analyzed with a ease. For figure 5.1 A dataset 1,2,3,4,5 are used and for 5.1 B dataset 11,12,13,14,15 are used provided in *Appendix E* with sample calculation*.*

Chapter 6
Conclusion and Recommendations

Identification and separation of different regimes encountered in many chemical engineering processes such as, flow regimes in two phase flow through a pipe, fluidized bed regimes in inverse fluidized bed, is the main objective of the project. One more study is added to work which shows the classification of the fluidization process if we vary the diameter and the density of the particles. A data set for both flow regimes through pipe fluidized bed regimes and for density and diameter variation situation was generated using appropriate correlations. Though the data was not predictable by seeing and it was too large as well, so classification was difficult but by using data driven methodology SVM and LDA it was done. By using both the techniques binary (two class) and multiclass separation is done.

Firstly classification is done for the flow regimes for two phase flow in a pipe. By taking any two regimes data classification (binary) is done and by taking all the class together multi classification is done. Similar work is done by using the same techniques for fluidized bed regimes named as packed bed regime, Semi fluidized bed regime and fully fluidized bed regime for an inverse fluidized bed.

For Gas fluidization one more aspect of density and diameter variation is studied and by using LDA classification of the data is done. The classification shows that within the range of a specified fluidization regime the quality of the fluidization can change still we have used already specified particles for the regime. The technique is appropriate for the classification of the data of particles having different density and diameter. By using this appropriate particles can be selected for the operation.

As both the techniques LDA and SVM seems easy to handle for this type of robust and too large data associated with many chemical engineering plant operations. We used it for the characterization of flow regimes for two phase flow in pipes and fluidized bed regimes in inverse fluidization. But as we see it is a useful chemometrictechnique which can be used for binary or multi classification of data in many processes where data handling is really an issue for identification and characterization of the data.

References

1*: Mandhane, J. M.; Gregory, G. A.; Aziz,* K.: A Flow PatternMap for Gas-Liquid Flow in Horizontal Pipes. Int. J. MultiphaseFlow**1974**, 1, 537-553.

2*: Theodore B. Trafalis,OlutayoOladunni, and Dimitrios V. Papavassiliou*: Two-Phase Flow Regime Identification with a Multi-classification Support Vector Machine (SVM) Model, Ind. Eng. Chem. Res. **2005**, 44, 4414-4426

3:*N. Ulaganathan, K. Krishnaiah*: Hydrodynamic characteristics of two-phase inverse fluidized bed, Bioprocess Engineering 15 (1996) 159 - 649 Springer-Verlag**1996**

4*: Martinez and A. Kak*: "PCA versus LDA", *IEEE Transactions on Pattern Analysis and Machine Intelligence*, vol. 23, no. 2, pp. 228-233, **2001**.

5: *Hsu, C.-W.; Lin, C.-J.*: A Comparison of Methods for Multi-classSupport Vector Machines. IEEE Trans. Neural Networks**2002**, 13, 415-425.

6: *Mi, Y.; Ishii, M.; Tsoukalas*, L. H.: Flow Regime IdentificationMethodology with Neural Networks and Two-Phase Flow Models.*Nucl.Eng. Des.***2001**, *204*, 87-100.

7: *McQuillan, K. W.; Whalley*, P. B.: Flow Patterns in VerticalTwo-Phase Flow. *Int. J. Multiphase Flow* **1985**, *11*, 161-175.

8*: Weisman, J.; Kang, S. Y.*:Flow Pattern Transitions inVertical and Upwardly Inclined Lines. *Int. J. Multiphase Flow*, 1981, *7*, 271-291

9: *Kaul, S.N.; Galakarli, S.K.*: Fluidized bed reactor for waste watertreatment, Chem. Engg. World, 15(2) (**1990**) 25-42

10: *Fan, L.S.*: Gas-Liquid-Solid fluidization engineering, Butterworths,Boston, (**1989**) 368-375

11: *R.J. FeminBendict, G. Kumaresan, M. Velan* :Bed expansion and pressure drop studies
in a liquid-solid inverse fluidised bed reactor, Bioprocess Engineering 19 (1998) (137-142) Springer-Verlag 1998

12:*Long Sang*: Particle Fluidization in Upward and Inverse Liquid-Solid Circulating Fluidized Bed, Doctor of Philosophy thesis, The University of Western Ontario , London, Ontario, Canada, 2013.

13: *George D. Cody, JayatiJohri, David Goldfarb:*Dependence of particle fluctuation velocity on gas flow, and particle diameter in gas fluidized beds for monodispersed spheres in the
Geldart B and A fluidization regimes, Powder Technology 182 (2008) 146–170.

Appendix A

Mat Lab Code for Linear Discriminant Analysis For Binary and Multi-Classification

```matlab
clc
clear all
% loading the data files

load dataset1.txt
load dataset2.txt
load dataset3.txt
load dataset4.txt
load dataset5.txt
% load dataset4.txt
% load dataset5.txt

save dataset1
save dataset2
save dataset3
save dataset4
save dataset5
% calculation of mean of each class

m1=mean(dataset1);
m2=mean(dataset2);
m3=mean(dataset3);
m4=mean(dataset4);
m5=mean(dataset5);
% overall mean

m=(m1+m2+m3+m4+m5)/5;

% class varience matrices

s1=cov(dataset1);
s2=cov(dataset2);
s3=cov(dataset3);
s4=cov(dataset4);
s5=cov(dataset5);

% within class matrix

Sw=s1+s2+s3+s4+s5;

% number of samples of each class

N2=size(dataset1,2);
N1=size(dataset2,2);
N3=size(dataset3,2);
N4=size(dataset4,2);
N5=size(dataset5,2);
```

```matlab
% beween class matrix

SB1 = N1*(m1-m)*(m1-m)';
SB2 = N2*(m2-m)*(m2-m)';
SB3 = N3*(m3-m)*(m3-m)';
SB4 = N4*(m4-m)*(m4-m)';
SB5 = N5*(m5-m)*(m5-m)';


SB = SB1+SB2+SB3+SB4+SB5;


% computing the LDA projections

inSw=inv(Sw);
inSw_by_SB=inSw*SB;

% getting the projection vectors

[V,D]=eig(inSw_by_SB);
W1=V(:,1);
W2=V(:,2);

% plotting of the scatter plot for visualisation

hfig=figure;
axes1=axes('Parent',hfig,'FontWeight','bold','FontSize',12);
hold ('all');
f1='the first feature';
f2='the second feature';

% xlable(f1)
% % ,'FontWeight','bold','FontSize',12);
% ylable(f2)
% ,'FontWeight','bold','FontSize',12);

% scatter of data and projection of mean of first class

scatter(dataset1(:,1),dataset1(:,2),'r','LineWidth',2,'Parent',axes1);
holdon

plot(m1(1),m1(2),'co','MarkerSize',8,'MarkerEdgeColor','c','Color','c','LineW
idth',2,'MarkerFaceColor','c','Parent',axes1);
holdon

% scatter of data and projection of mean of second class

scatter(dataset2(:,1),dataset2(:,2),'y','LineWidth',2,'Parent',axes1);
holdon

plot(m2(1),m2(2),'mo','MarkerSize',8,'MarkerEdgeColor','m','Color','m','LineW
idth',2,'MarkerFaceColor','m','Parent',axes1);
holdon
```

```matlab
% scatter of data and projection of mean of third class

scatter(dataset3(:,1),dataset3(:,2),'b','LineWidth',2,'Parent',axes1);
hold on

plot(m3(1),m3(2),'yo','LineWidth',2,'MarkerSize',8,'MarkerEdgeColor','y','Col
or','y','LineWidth',2,'MarkerFaceColor','y','Parent',axes1);
hold on

% scatter of data and projection of mean of fourth class

scatter(dataset4(:,1),dataset4(:,2),'g','LineWidth',2,'Parent',axes1);
hold on

plot(m4(1),m4(2),'ro','LineWidth',2,'MarkerSize',8,'MarkerEdgeColor','r','Col
or','r','LineWidth',2,'MarkerFaceColor','r','Parent',axes1);
hold on

% scatter of data and projection of mean of fifth class

scatter(dataset5(:,1),dataset5(:,2),'v','LineWidth',2,'Parent',axes1);
hold on

plot(m5(1),m5(2),'go','LineWidth',2,'MarkerSize',8,'MarkerEdgeColor','g','Col
or','g','LineWidth',2,'MarkerFaceColor','g','Parent',axes1);
hold on
```

Appendix B

The MATLAB swSVMSoftware

We have a programmed a simple SVM implementation in MATLAB. The example and the figures in the preceding pages where obtained using this software. There are only two choices for the kernel function that have been implemented, namely, Gaussian RBF and Linear.

Description of the Functions

There are five MATLAB functions, and by their function we have broken them into three categories.

Functions for SVM Training and Classification

There are three functions that implement the SVM- *swSVM*, *swquad*and*swSVMclassify*. The function that solves the QP for obtaining the SVM solution is swquad. The function *swSVMclassify*classifies test patterns, using the solution obtained previously by *swquad*. The function*swSVM*is like a main function that accepts as inputs the training patterns and their labels; the test patterns, the choice of the kernel and the sigma parameter (only needed for the RBF kernel). It calls *swquad*for solving the Quadratic Program to perform SVM separation and then calls *swSVMclassify*, which classifies the test patterns. If the data are two dimensional, *swSVM* also plots the training patterns, the margin and the decision boundary by calling *swPlot*.

Plotting Related Functions

The function *swScatter*does a scatter plot of the training patterns; and it outputs the patterns of category 1 as blue plus markers and the patterns of category 2 as red asterisk. (We assign y=1 to the patterns of category 1 and y= -1 to the patterns of category 2, but this can be reversed with no loss of generalization). The function *swPlot*is used to plot the training patterns and the decision boundary as well as the margin of the SVM. This function uses the outputs of the *swquad* function. The function *swPlot* calls the function *swScatter*.

Helper functions

There is one helper function *swScale*, which is called by other functions for scaling the training patterns before plotting the margin and decision boundaries.A Sample Session of the *swSVM* MATLAB software.

Mat Lab Code for Binary Classification

```matlab
clc;
clearall;
closeall;

% loading the data files

load('fully.txt');
load('semi.txt');

% making data files from source files

data1=[fully(:,1),fully(:,2)];
data2=[semi(:,1),semi(:,2)];
data=[data1;data2];
x=data(:,1);
y=data(:,2);

% loop for the classification

fori=1:40
if(i<=20)
c(i)={'fully'};
else
c(i)={'semi'};
end
end
c=c';

% defining parameters (SVM algorithm)

kerneltype='rbf';
groups = ismember(c,'fully');
[train, test] = crossvalind('holdOut',groups);

cp = classperf(groups);
svmStruct = svmtrain(data(train,:),groups(train),'showplot',true);
sigma=1;

alpha=svmStruct.Alpha;

Xs=svmStruct.SupportVectors(:,1);
Ys=svmStruct.SupportVectors(:,2);
```

```
[W0,b0,alpha]=swquad(x,y,Xs,Ys,kerneltype,sigma);
figure;

swPlot(x,y,'rbf',alpha, W0,b0 ,sigma);
class=swSVMclassify(alpha, b0, x,y,test,kerneltype,sigma)
```

This part of appendix contains the Multi-classification SVM flow pattern transition classifiers for vertical and horizontal flow regime maps. The flow pattern class is in parentheses (+1or-1).

MSVM, P=1, C=1 Classifiers for Vertical Flow Regimes

Bubble (+1)-intermittent (-1) flow transition

$f(x) = \text{sign}(-1.6546 \ln(v_{SG}) + 1.3053 \ln(v_{SL}) - 0.4277$

Intermittent (+1)-annular (-1) flow transition

$f(x) = \text{sign}(-1.8081 \ln(v_{SG}) +0.0798 \ln(v_{SL})+ 4.1069$

MSVM, P=2, C=0.1 Classifiers for Vertical Flow Regimes.

Bubble (+1)-intermittent (-1) flow transition

$f(x) = \text{sign}(-0.8382 \ln(v_{SG})+0.8919 \ln(v_{SL})-0.0596 \ln(v_{SG}) \ln(v_{SL})$

$$+0.0516 \ln(v_{SG})^2 + 0.1725 \ln(v_{SL})^2- 0.8166$$

Intermittent (+1)-annular (-1) flow transition

$f(x) = \text{sign}(-0.0673 \ln(v_{SG})-0.0701 \ln(v_{SL})+0.0933 \ln(v_{SG}) \ln(v_{SL})$

$$-0.3962 \ln(v_{SG})^2 + 0.0475 \ln(v_{SL})^2+ 2.1867$$

Appendix C

Data table

Parameter	Value
Density liquid	996
Density gas	1.17
Surface tension	0.0728
g	9.8
Diameter	0.0254
Viscosity liquid	0.001
Viscosity gas	0.00016

Sample calculation for one data set

In this operation all flow regimes appears with specific gas and liquid velocities which can be taken in consideration as Reynolds number. When the gas flows as laminar the flow regime is generally the bubble dispersed flow, with transition gas flow the flow regime is intermittent flow and with turbulent flow of gas, the regime is annular.

For Gas laminar flow, taking Reynolds no as 700

$$Re = \rho_g v D / \mu_g$$

on putting all the values in the equation

$V_G = 3.76$ m/sec

Now using this gas velocity value in the bubble dispersed flow correlation

$$V_L = 3.0 * V_G^{-1.15}[\, g \, \sigma \, (\rho_L - \rho_G) \, / \, \rho_L^2 \,]^{1/4}$$

$V_L = 1.39$ m/sec

Similarly all the datasets can be generated.

Data sets for Two Phase Flow through pipes

Bubble Dispersed Flow

V_L (m/s)	V_G (m/s)
1.336843	2.827056
1.337107	2.827847
1.337371	2.828637
1.337634	2.829428
1.337898	2.830219
1.338161	2.831009
1.338425	2.8318
1.338688	2.83259
1.338952	2.833381
1.339215	2.834171
1.339479	2.834962
1.339742	2.835752
1.340006	2.836543
1.340269	2.837334
1.340533	2.838124
1.340796	2.838915
1.34106	2.839705
1.341323	2.840496
1.341587	2.841286

Intermittent flow

V_L (m/s)	V_G (m/s)
1.536843	7.97641
1.57107	7.9772
1.537371	7.977991
1.537634	7.978781
1.537898	7.979572

1.538161	7.980362
1.538425	7.981153
1.538688	7.981944
1.538952	7.982734
1.539215	7.983525
1.539479	7.984315
1.539742	7.985106
1.540006	7.985896
1.540269	7.986687
1.540533	7.987477
1.540796	7.988268
1.54106	7.989059
1.541323	7.989849
1.541587	7.99064

Annular flow

V_G(m/s)	V_L (m/s)
14.58207147	1.97641
14.66308298	1.9772
14.74409449	1.977991
14.825106	1.978781
14.9061175	1.979572
14.98712901	1.980362
15.06814052	1.981153
15.14915203	1.981944
15.23016354	1.982734
15.31117505	1.983525
15.39218655	1.984315
15.47319806	1.985106
15.55420957	1.985896

15.63522108	1.986687
15.71623259	1.987477
14.71169	1.988268
14.72249	1.989059
14.73329	1.989849
14.74409	1.99064

Appendix D

Data Table

Property	Range
Particle diameter (mm)	12.5, 12.9, 20
Particle density (kg/m³)	126, 216, 380, 534
Initial bed height (m)	0.23-0.79
Superficial gas velocity (m/sec)	0.02-0.15
Voidage of packed bed	0.52, 0.524, 0.545

Data sets for Fluidized Bed regimes

Sample calculation for one dataset

For packed bed fluidized bed

For packed bed situation there is a specific range of Reynolds number i.e.; $325 < Re < 2100$

Let's take Re = 500

Using relation $Re = \rho_p * U * d_p/\mu$

On putting all values U = 0.28 m/sec

Using friction factor relation

$$f = 60 * Re_m^{-0.415}$$

f= 3.35

Now using pressure drop correlation

$$f = [(\Delta P) * d_p * \frac{e_p^3}{\rho U^2} * H_p * (1 - \varepsilon_p)]$$

On putting all the values in the correlation $\Delta P = 2.8 \ n/m^2$

Packed bed Fluidized bed regime

U (m/s)	Pressure Drop (N/m^2)
0.025	2.2
0.026	2.4
0.027	2.6
0.028	2.8
0.029	3
0.03	3.2
0.031	3.4
0.032	3.6
0.033	3.8
0.034	4
0.035	4.2
0.036	4.4
0.037	4.6
0.038	4.8
0.039	5
0.04	5.2
0.041	5.4
0.042	5.6
0.043	5.8
0.044	6

Semi Fluidized bed regime

U (m/s)	Pressure Drop (N/m^2)
0.071	8.2
0.072	8.4
0.073	8.6
0.074	8.8
0.075	9

0.076	9.2
0.077	9.4
0.078	9.6
0.079	9.8
0.08	10
0.081	10.2
0.0815	10.4
0.082	10.6
0.083	10.8
0.084	11
0.085	11.2
0.086	11.4
0.087	11.6
0.088	11.8
0.09	12

Fully Fluidized bed regime

U (m/s)	Pressure Drop (N/m^2)
0.12	17.1
0.1205	17.2
0.121	17.3
0.1215	17.4
0.122	17.5
0.1225	17.6
0.123	17.7
0.1235	17.8
0.124	17.9
0.1245	18
0.125	18.1
0.1255	18.2

0.126	18.3
0.1265	18.4
0.127	18.5
0.1275	18.6
0.128	18.7
0.1285	18.8
0.129	18.9
0.13	19

Appendix E

Data Table for different particles

Measurement	ρ_p g $/cm^3$	μ_f $\mu poise$	D μm	D_b^0 μm	U_{mf}^* cm /s	$\emptyset_{mf}$	n
ASN Glass R87	2.45	210	149	128	1.6	0.613	4.718
ASN Glass R63	2.45	210	210	121	3.7	0.597	4.765
ASN Polymer 1	1.04	210	320	174	3.5	0.601	4.735
ASN Polymer 2	1.04	210	650	178	10.0	0.640	4.639
ASN Nickel	8.9	181	76	44.8	4.27	0.511	5.025

Sample calculation for one data set

$$U_{mf}^* = [\frac{(1-\emptyset_{mf})^3}{150\,\emptyset_{mf}}](\frac{D^2\rho_p g}{\mu_f}) \qquad 1$$

$$U_t = [\frac{D^2\rho_p g}{18\mu_f}] \qquad 2$$

$$U_s = (1-\emptyset)^n U_t \qquad C$$

By using first two equations,

$$U_{mf}^* = \left[\frac{(1-\emptyset_{mf})^3}{\emptyset_{mf}}\right] * \frac{3}{25} * U_t \qquad D$$

putting all the values in equation C and D in SI unit values can be calculated.

Calculation for U_t

$$U_t = \frac{[(149 * 10^{-6})^2 * (2.45 * 10^3) * 9.8]}{18 * 210 * 10^{-6}}$$

$$U_t = 0.141\ m/sec$$

Using this U_t value, corresponding U_{mf} and U_s values can be calculated. $U_{mf} = 0.00159$, $U_s = 0.0015$ m/s.

Dataset1(ASN Glass R87)

U_S(m/s)	U_{mf}(m/sec)
0.0015	0.00159
0.00155	0.0016
0.0016	0.00161
0.00165	0.00162
0.0017	0.00163
0.00175	0.00164
0.0018	0.00165
0.00185	0.00167
0.0019	0.00168
0.00195	0.00169

Dataset2 (ASN Glass R63)

U_S(m/s)	U_{mf}(m/sec)
0.00368	0.0036
0.00367	0.00361
0.00369	0.00362
0.0037	0.00363
0.00371	0.00364
0.00372	0.00365
0.00373	0.00366
0.00374	0.00367
0.00375	0.00368
0.00376	0.00369

Dataset3 (ASN Polymer 1)

U_S(m/s)	U_{mf}(m/sec)
0.0035	0.00356
0.00351	0.00357
0.00352	0.00358
0.00353	0.00359
0.00354	0.0036
0.00355	0.00361
0.00356	0.00362
0.00357	0.00363
0.00358	0.00364
0.00359	0.00365

Datase4 (ASN Polymer 2)

U_S(m/s)	U_{mf}(m/sec)
0.0035	0.00356
0.00351	0.00357
0.00352	0.00358
0.00353	0.00359
0.00354	0.0036
0.00355	0.00361
0.00356	0.00362
0.00357	0.00363
0.00358	0.00364
0.00359	0.00365

Dataset5 (ASN Nickel)

U_S(m/s)	U_{mf}(m/sec)
0.0042	0.00422
0.00421	0.00423
0.00422	0.00424

0.00423	0.00425
0.00424	0.00426
0.00425	0.00427
0.00426	0.00428
0.00427	0.00429
0.00428	0.0043
0.00429	0.00431

Dataset11

U_S(m/s)	U_{mf}(m/sec)
1.06	0.0015
1.032258065	0.00155
1.00625	0.0016
0.981818182	0.00165
0.958823529	0.0017
0.937142857	0.00175
0.916666667	0.0018
0.902702703	0.00185
0.884210526	0.0019
0.866666667	0.00195

Dataset12

U_S(m/s)	U_{mf}(m/sec)
0.97826087	0.00368
0.983651226	0.00367
0.98102981	0.00369
0.981081081	0.0037
0.981132075	0.00371
0.981182796	0.00372
0.981233244	0.00373
0.981283422	0.00374

U_S(m/s)	U_{mf}(m/sec)
0.981333333	0.00375
0.981382979	0.00376

Dataset13

U_S(m/s)	U_{mf}(m/sec)
1.017142857	0.0035
1.017094017	0.00351
1.017045455	0.00352
1.016997167	0.00353
1.016949153	0.00354
1.016901408	0.00355
1.016853933	0.00356
1.016806723	0.00357
1.016759777	0.00358
1.016713092	0.00359

Dataset14

U_S(m/s)	U_{mf}(m/sec)
1.1	0.009
1.10989011	0.0091
1.108695652	0.0092
1.107526882	0.0093
1.106382979	0.0094
1.105263158	0.0095
1.104166667	0.0096
1.103092784	0.0097
1.102040816	0.0098
1.101010101	0.0099

Dataset15

U_S(m/s)	U_{mf}(m/sec)
1.179775281	0.0042

1.179271709	0.00421
1.17877095	0.00422
1.178272981	0.00423
1.177777778	0.00424
1.177285319	0.00425
1.17679558	0.00426
1.17630854	0.00427
1.175824176	0.00428
1.175342466	0.00429